VII. ELECTRON MAGNETIC RESONANCE*

Academic and Research Staff

Prof. K. W. Bowers

Graduate Students

Nancy H. Kolodny
C. Mazza
A. C. Nelson
R. S. Sheinson
N. S. Suchard
Y-M. Wong
B. S. Yamanashi

A. EXCITED STATES

Electron spin resonance measurements of zero-field splittings (ZFS) will be discussed briefly in terms of the molecular geometry of excited states in which total spin S = 1, 3/2, 2, 5/2, etc. For example, ZFS of biphenyl-like molecules in the S = 1 emitting state can be treated as a function of the dihedral angle θ_d. The trend of the ZFS with varying θ_d $(0 \rightarrow \pi/2)$ is computed on the basis of a simple model with double "1/2 electron" delta functions and Häckel MO coefficients and is found to be in agreement with the trend observed from the 22'-bridged biphenyl-like systems.

1. General Discussion

The ZFS in general has the form[1]

$$\langle {}^{2|S|+1}\Psi(r_1,\ldots,r_n)\ |\hat{U}(r_{ij})|\ {}^{2|S|+1}\Psi(r_1,\ldots,r_n)\rangle \tag{1}$$

and constitutes the eigenvalues of the spin Hamiltonian at zero external field. The functional notations ${}^{2|S|+1}\Psi(r_1,\ldots,r_n)$ and $\hat{U}(r_{ij})$ represent the spatial function of a $2|S|+1$ multiplet system with n unpaired electrons whose coordinates are labeled $\{r_1,r_2,\ldots,r_n\}$, and the electron-electron spin dipolar operator, r_{ij} is the inter-electronic distance $|r_i-r_j|$. The form of the integral (1) does not lose generality even when spin-orbit coupling is appreciable in the total spin Hamiltonian.[2] In such a situation the effective spin operator is defined by means of first-order perturbation theory which takes spin-orbit coupling into consideration and forms a new set of eigenkets.

The electron-electron contact interaction within a multiplet is a constant

$$\xi(r_{ij}) = -\frac{8\pi}{3} g^2\beta^2 \sum_{i<j} \delta(r_{ij})\ \bar{s}_i \cdot \bar{s}_j, \tag{2}$$

where δ is a Dirac delta function and only causes the levels of zero-field eigenvalues

*This work was supported by the Joint Services Electronics Programs (U.S. Army, U.S. Navy, and U.S. Air Force) under Contract DA 28-043-AMC-02536(E).

to be shifted uniformly. This does not alter the ZFS. The electron-nuclear contact hyperfine interaction,

$$\hat{H}_{hfs} = \bar{s} \cdot \left(\sum_{i,k} \rho_i \bar{A}_{ik} \right) \cdot \bar{I} \tag{3}$$

where the central term in the product is a hyperfine tensor which is dependent upon the density of unpaired electrons, ρ_i, at the nuclei. The magnitude of (3) is $10^{-2} \sim 10^{-3}$ of that of electron-electron spin dipolar interaction which is the dominant cause of ZFS.[3] The spin dipolar term can be written with the phenomenological spin[4] operator $\bar{S}$ as

$$\hat{H}_{dip} = -2^{-1} g^2 \beta^2 \sum_{u=x,y,z} \langle 3u_{ij}^2 - r_{ij}^2 / r_{ij}^5 \rangle \bar{S}_u^2, \tag{4}$$

where x, y, and z are the principal axes about which symmetry operation (elements) of the point group to which the system belongs leaves the Hamiltonian invariant. The symbol $\langle\ \rangle$ in Eq. 4 denotes the expectation value of $\left[3u_{ij}^2 - r_{ij} \right] r_{ij}^{-5}$ over the spatial function $^{2|S|+1}\Psi(r_1, \ldots, r_n)$ which can be computed as the resultant vector of configuration interactions.[5]

$$| {}^{2|S|+1}\Psi(r_1, \ldots, r_n) \rangle = \sum_i c_i \psi_i, \tag{5}$$

where the ψ_i's are LCAO MO's such that

$$\psi_j = \sum_j b_j a_j. \tag{6}$$

Thus if g(r) is some geometrical parameter characteristic of a $2|S|+1$ multiplet state, the dependence of the ZFS upon the parameter g(r) can be treated as

$$\psi_j(g(r)) = \sum_j b_j(g(r))\, a_j, \tag{7}$$

and then the spatial part of the multiplet vector becomes

$$| {}^{2|S|+1}\Psi(r_1, \ldots, r_n) \rangle = \sum_i \sum_j c_i b_i(g(r))\, a_j. \tag{8}$$

2. Computation of ZFS for Twisted Biphenyls

For a specific example of the g(r) dependence, a biphenyl with a dihedral angle θ_d is discussed. Let

$$g(r) = \theta_d(r). \tag{9}$$

The simplest reasonable assumption for the 1, 1' twisted molecule is[6]

$$\begin{cases} \theta_d(r) = \cos^{-1} \beta_{11'}(r) & (10) \\ 0 = \cos^{-1} \beta_{ij}(r), \qquad i \neq 1, \; j \neq 1' & (11) \end{cases}$$

where the β_{ij} are the resonance integrals between i^{th} and j^{th} atoms (see Fig. VII-1).

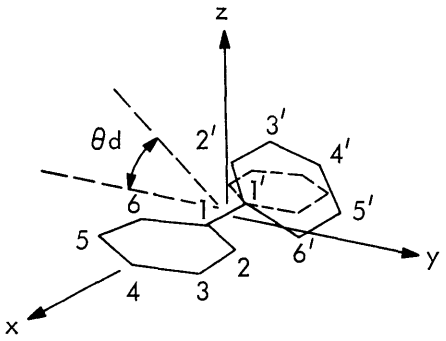

Fig. VII-1. Dihedral angle θ_d and labeling of atomic positions in biphenyl.

For the S = 1 state only the singly excited configuration of the lowest energy is assumed to comprise the lowest triplet state. Equation 8 then takes a simple form[7]

$$|{}^3\Psi_o(\theta_d)\rangle = 2^{-1/2} \, |\psi(\theta_d, 1)\psi'(\theta_d, 2) - \psi(\theta_d, 2)\psi'(\theta_d, 1)\rangle, \tag{12}$$

where 1 and 2 are labels of the coordinates of electrons 1 and 2, and

$$\psi(\theta_d, n) = \sum_i b_i(\theta_d) \, a_i(n), \qquad \psi'(\theta_d, n) = \sum_i b'_i(\theta_d) \, a_i(n), \qquad n = 1, 2$$

where $\psi(\theta_d, n)$ and $\psi'(\theta_d, n)$ are the highest bonding and the lowest antibonding MO's.

Substitution of (13) in (12) and the subsequent substitution of the result in (1) gives

$$\langle {}^3\Psi_o(\theta_d, 1, 2) \, |\hat{U}(r_{12})| \, {}^3\Psi_o(\theta_d, 1, 2)\rangle = \langle \psi(\theta_d, 1)\,\psi'(\theta_d, 2) - \psi(\theta_d, 2)\,\psi'(\theta_d, 1) \, |\hat{U}(r_{12})| \, \psi(\theta_d, 1)\,\psi'(\theta_d, 2)\rangle$$

$$= \int_2 \int_1 \sum_i \sum_j b_i(\theta_d) \, b_j(\theta_d) \, a_i(1) \, a_j(1) \, \hat{U}(r_{12}) \sum_k \sum_\ell b'_k(\theta_d) \, b'_\ell(\theta_d) \, a_k(2) \, a_\ell(2) \, dv_1 dv_2$$

$$- \int_2 \int_1 \sum_i \sum_j b_i(\theta_d) \, b'_j(\theta_d) \, a_i(1) \, a_j(1) \, \hat{U}(r_{12}) \sum_k \sum_\ell b_k(\theta_d) \, b'_\ell(\theta_d) \, a_k(2) \, a_\ell(2) \, dv_1 dv_2. \tag{14}$$

Now, in order to account for the effect of the change in the dihedral angle upon the z component of spin-spin interaction in a simple manner, AO's are conceived as

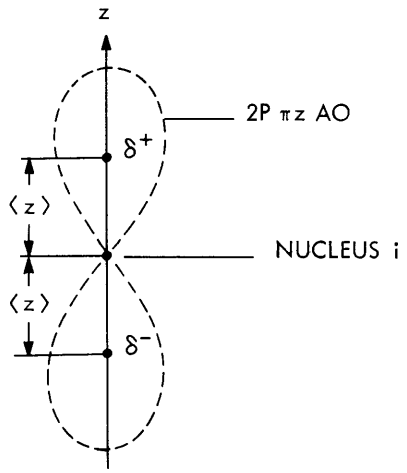

Fig. VII-2. Dewar-type "1/2 electron" double-delta function and the distance ⟨z⟩ from the nucleus i.

consisting of two delta functions[8, 9] (see Fig. VII-2)

$$a_i(n) = 2^{-1/2}\left[\delta_i^+(n) - \delta_i^-(n)\right], \qquad n = 1, 2, \tag{15}$$

in which the superscript minus sign comes from the π symmetry, and each Dewar-type "1/2 electron" is located at an average distance $\langle z \rangle$ from the i^{th} nucleus

$$\langle z \rangle = \iint \psi_{2pz}^{*}\, z\, \psi_{2pz}\, dv dv'. \tag{16}$$

Substitution of (15) in (14) gives

$$\langle {}^3\Psi_o(\theta_d, 1, 2) \left| \hat{U}(r_{12}) \right| {}^3\Psi_o(\theta_d, 1, 2) \rangle = I(\theta_d, 1, 2)$$

$$= \int_2 \int_1 \sum_i \sum_j b_i(\theta_d)\, b_i(\theta_d)\, 2^{-1} \left\{\delta_i^+(1) - \delta_i^-(1)\right\} \left\{\delta_j^+(1) - \delta_j^-(1)\right\} \hat{U}(r_{12}) \sum_k \sum_\ell b'_k b_\ell \left\{\delta_k^+(2) - \delta_k^-(2)\right\}$$

$$\times \left\{\delta_\ell^+(2) - \delta_\ell^-(2)\right\} dv_1 dv_2 - \int_2 \int_1 \sum_i \sum_j b_i(\theta_d)\, b'_j(\theta_d)\, 2^{-1} \left\{\delta_i^+(1) - \delta_i^-(1)\right\}$$

$$\times \left\{\delta_j^+(1) - \delta_j^-(1)\right\} \hat{U}(r_{12}) \sum_k \sum_\ell b'_k(\theta_d)\, b'_i(\theta_d)\, 2^{-1} \left\{\delta_k^+(2) - \delta_k^-(2)\right\}$$

$$\times \left\{\delta_\ell^+(2) - \delta_L^-(2)\right\} dv_1 dv_2, \tag{17}$$

where $\delta_i^{\pm}(n)\,\delta_j^{\pm}(n)$, $\delta_k^{\pm}(n)\,\delta_\ell^{\pm}(n) = 0$, $i \neq j$, $k \neq \ell$.

Equation 17 reduces to

$$I(\theta_d, 1, 2) = \sum_i \sum_k b_i(\theta_d)\, b'_k(\theta_d)\, \{b_i(\theta_d) b'_k(\theta_d) - b_k(\theta_d) b'_i(\theta_d)\}$$

$$\times \left[\{\hat{U}(r_{12})\}_{i_1^+ k_2^+} + \{\hat{U}(r_{12})\}_{i_1^+ k_2^-} + \{\hat{U}(r_{12})\}_{i_1^- k_2^+} + \{\hat{U}(r_{12})\}_{i_1^- k_2^-} \right], \qquad (18)$$

where $\{\hat{U}(r_{12})\}_{i_1^+ k_2^-}$ denotes, for example, $\hat{U}(r_{12})$ evaluated with electron 1 at nuclear site i, (+) position (above the phenyl plane), and with electron 2 at nuclear site k, (-) position (below the phenyl plane).

The approximations (15) → (18) mean that spin dipolar interactions among $2p\pi$ AO's are replaced by those among point charges above and below the phenyl plane, and the distance of these charges from the nuclei to which they belong is taken as $\langle z \rangle$. The charges above and below the plane at each nuclear site are weighted with AO coefficients. The definition of delta function excludes the possibility of electron n belonging to i^{th} and j^{th} nuclear sites simultaneously. The ZFS parameters D and E and the principal values X, Y, and Z are proportional to the value of (18) when operator $\hat{U}(r_{12})$ is defined as

$$\hat{U}(r_{12}) \equiv 4^{-1} g^2 \beta^2 r_{12}^{-5} \begin{pmatrix} r_{12}^2 - 3z_{12}^2 \\ 3y_{12}^2 - 3x_{12}^2 \end{pmatrix} \quad \text{for} \quad \begin{pmatrix} D \\ E \end{pmatrix}, \qquad (19)$$

and

$$\hat{U}(r_{12}) \equiv -2^{-1} g^2 \beta^2 r_{12}^{-5} \left[r_{12}^2 - 3 \begin{pmatrix} x_{12}^2 \\ y_{12}^2 \\ z_{12}^2 \end{pmatrix} \right] \quad \text{for} \quad \begin{pmatrix} X \\ Y \\ Z \end{pmatrix}. \qquad (20)$$

3. Experiment

The experimental ZFS are taken for biphenyl, 9,10-dihydrophenanthrene, 1,2,3,4-dibenz-1,3-cycloheptadiene-6-one, and 1,2,3,4-dibenz-1,3-cyclo-octadiene-6-one. (The last three compounds are referred to in Fig. VII-4c as A, B, and C.)

All EPR from which ZFS were determined were taken on a Varian E-3 X-band (~3 cm) EPR spectrometer with the following settings: scan range, 5×10^3 Oe; field setting, 2.5×10^3 Oe; time constant, 3×10^{-1} sec; scan time, 4 ~ 8 min; modulation

amplitude, 20 Oe; modulation frequency, 10^2 kHz; receiver gain, $5 \sim 10 \times 10^5$; temperature of the sample, 77°K; microwave power, 0.5 ~ 1.6 mW; and microwave frequency, ~9.24 ± 0.005 GHz. Samples were prepared by dissolving ~0.015 g of solid compounds (several times recrystalized and sublimed) into 3 ml of EPA, a portion of which was transferred into a quartz sample tube, degassed three to five times, and vacuum sealed. The sample tube was then immersed in the liquid nitrogen contained in the specially designed dewar (Varian V-4546 modified to facilitate frequent evacuation) for allowing ultraviolet irradiation on the sample while the spectrum was taken. For the UV irradiation of the sample a Hanovia 10^3 W Hg-Xe high-pressure compact arc (Cat No. 5378) with Shoeffel (1 H-151 H) housing with reflector and collimator was used. The arc was operated at 60 V, 18 A. A water-filled quartz filter was placed between the UV arc and the microwave cavity to filter out IR emission of the arc.

4. Results

ZFS of twisted biphenyls as functions of the dihedral angle θ_d are shown in Figs.VII-3 and VII-6. The computed value $D_{av}E_{av}$ are the relative ZFS and the factor $\sim 1.6 \times 15^{-1}$ is required to convert them into D and E parameters in units of cm^{-1}.

The computed trend of the rapidly increasing E_{av} (Fig. VII-3a) and slowly decreasing

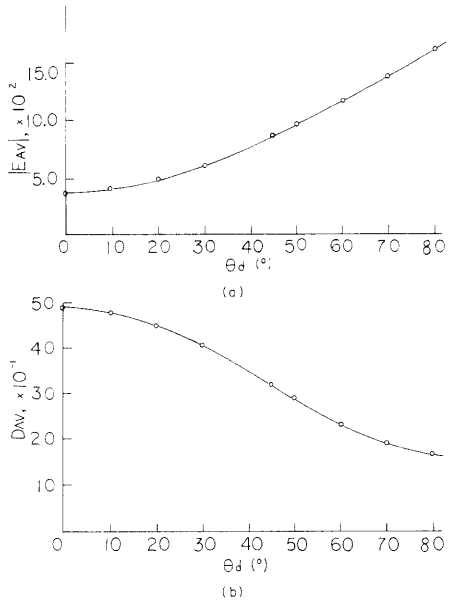

Fig. VII-3.
(a) Trend of E parameter calculated for biphenyl with increasing dihedral angle.
(b) Trend of D parameter calculated for biphenyl.

D_{av} (Fig. VII-3b) as the dihedral angle, θ_d, varies from $0 \rightarrow \pi/2$ agrees with the trends of D and E observed (Fig. VII-4a and -4b) with twisted compounds A ($\theta_d \approx 20°$), B ($\theta_d \approx 52°$), and C ($\theta_d \approx 85°$). The observed stationary resonance fields, (SRF), are shown in Fig. VII-4c (only the lower field $\Delta M_s = \pm 1$ fields are shown). The canonical

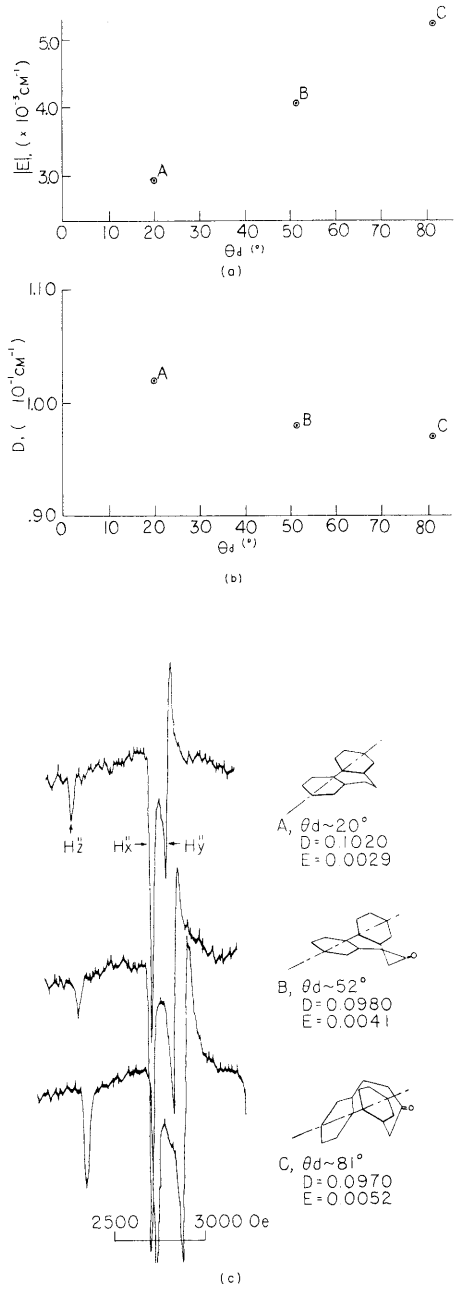

Fig. VII-4. (a) Experimental E value for compounds A, B, and C.
(b) Experimental D value for compounds A, B, and C.
(c) Electron magnetic resonance spectra, lower ΔM_s = ±1 canonical fields, of compounds A, B, and C.

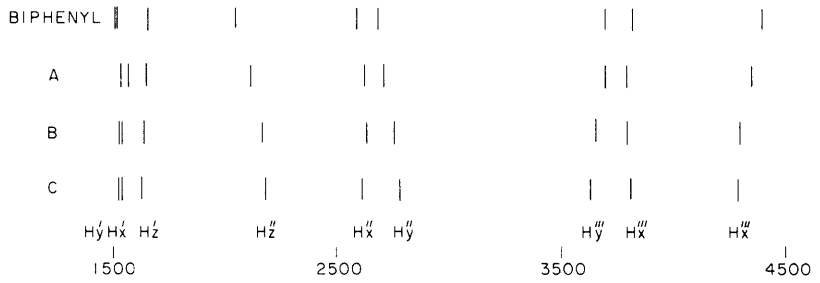

Fig. VII-5. Canonical stationary resonance fields (H_{min} not included) computed from observed ZFS by use of Kottis-Lefèbvre expression $F(\delta, H) = f(\theta, \phi)$, $\delta = 9.130$ GHz.

Table VII-1. Ratios of zero-field splittings and principal values of compound A, B, C and biphenyl and dihedral angle θ_d.

Compounds / Parameters	A	Biphenyl	B	C
D/E	35.17	31.44	23.90	18.65
X/Y	1.186	1.211	1.288	1.384
X/Z	.543	.547	.563	.580
Y/Z	.457	.452	.437	.420
θ_d	~20°	—	~52°	~81°

SRF computed from the ZFS observed by means of the resonance condition are indicated in Fig. VII-5 and Table VII-1.

The computed principal values X_{av}, Y_{av}, and Z_{av} are plotted against θ_d in Fig. VII-6. The dark dots were calculated from Eq. 18 by using the expectation value of z (that is, Eq. 16), while the open circles were computed from the same equation (18), but the most probable value of the 2pz electron in the z direction was used ($\langle z \rangle = 0.472$, $(z)_{\text{most prob}} = 0.504$). Y_{av} and Z_{av} change with respect to θ_d in a nearly mirror-image fashion, whereas X_{av} behaves almost linearly. These reflect the nature of twisting (axial twist along x) and the symmetry of the system (D_2). The observed trend of X, Y, and Z is shown in Fig. VII-7. Notice that the value of X approaches that of Y as $\theta_d \rightarrow \pi/2$. This means that the spin dipolar interaction in orthogonally twisted biphenyl is very similar to that of two nearly independent D_{6h} systems.

The squares of AO's at nuclear positions 1, 2, 3, and 4 are plotted against θ_d in Fig. VII-8. Here, the AO's that are located close to the twist site are more rapidly changing with respect to the AO's that are farther apart from the site as θ_d varies from

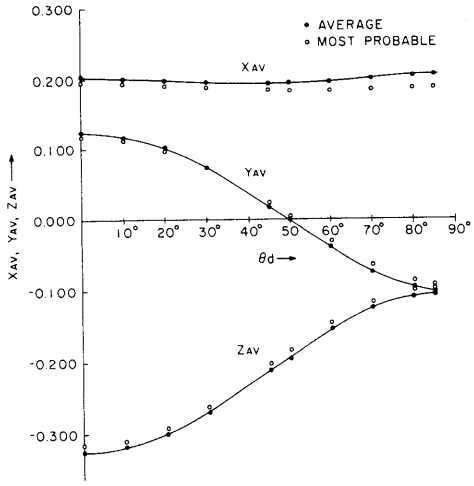

Fig. VII-6.

Behavior of zero-field eigenvalues computed for biphenyl with increasing dihedral angle.

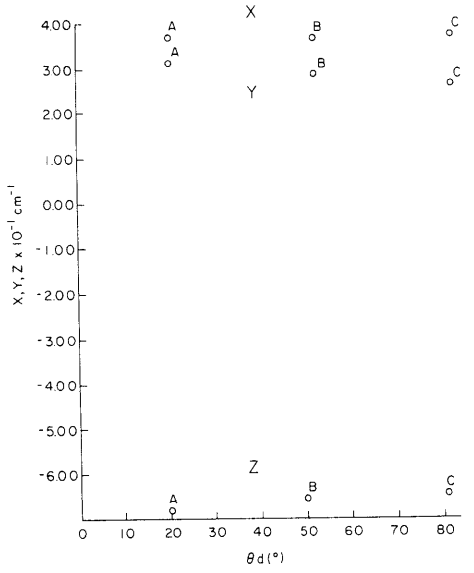

Fig. VII-7.

Experimental zero-field energies for X, Y, and Z.

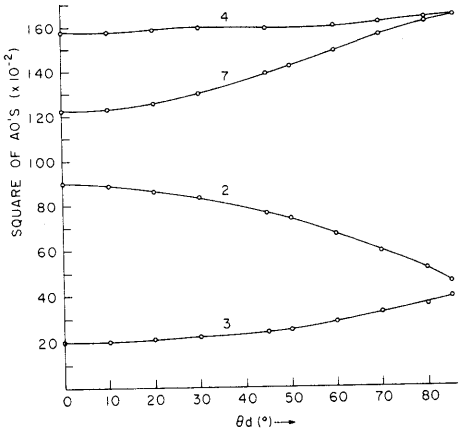

Fig. VII-8.

Square of AO's at positions 1, 2, 3, and 4 vs dihedral angle for the highest filled and the lowest unfilled MO's.

$0 \rightarrow \pi/2$. The behavior of AO's of the system with θ_d near $\pi/2$ is more like that of benzene than of biphenyl, as expected.

5. Conclusions

1. Zero-field splittings of molecules in $2|S|+1$, $S \neq 0$ multiplet state must reflect the intramolecular geometry characteristic of the state in an orderly manner.

2. ZFS of randomly oriented biphenyl-like molecules is a well-behaved function of the dihedral angle, θ_d.

3. The molecular symmetry and the change in the intramolecular geometry are better reflected when the ZFS are expressed as principal values X, Y, and Z and plotted against g(r) than when the conventional D and E are used.

4. The behavior of AO coefficients for the "highest filled" and the "lowest unfilled" MO's is consistent with a decreasing plane-to-plane and increasing in-plane dipolar interaction of triplet spins as θ_d increases $(0 \rightarrow \pi/2)$.

5. A very simple model, "1/2 electron" double-delta functions with simple Häckel MO's without configuration interaction or many-centered atomic integrals accounts reasonably for the trend of ZFS with varying θ_d.

6. Discussion

a. Use of the Double-Delta Function Model

We wished to see whether a simple point-charge model would successfully predict the trend of ZFS with respect to the dihedral angle. The intention was not so much to compute the exact value of ZFS itself as to predict the trend of variation in a series of molecules that differ only in geometry, such as the 2-2'-bridged twisted biphenyls or methyl-substituted naphthalenes. The simplest possible approach would have been to take each AO as a delta function located at the nucleus. In the case of twist systems, however, it was important to construct a model in which the contribution to the ZFS at the 1-1' bond would be particularly sensitive to the twist angle.

b. Orbital Degeneracy as a Function of Twist Angle

As the angle of twist changes from 0 to $\pi/2$ the HMO eigenvalues change (as shown in Fig. VII-9), orbitals 1 and 2 become doubly degenerate, and orbitals 3, 4, 5, and 6 form a fourfold degeneracy. The energy levels at $\theta_d = \pi/2$ is an extrapolation of the trend computed from 0° up to 85°. The eigenvalues for several angles are shown in Table VII-2. The spectrum of bimesytyl (see Fig. VII-10),

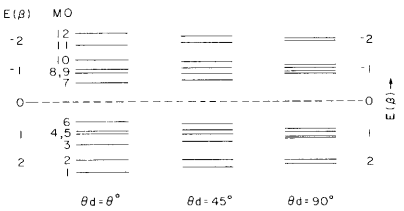

Fig. VII-9. Trend of eigenvalues with respect to change in dihedral angle.

Table VII-2. Eigenvalues of biphenyl with respect to the dihedral angle, θ_d.

MO \ θ_d	0°	10°	20°	30°	45°	50°	60°	70°	80°	85°
1	2.2784	2.2721	2.2539	2.2252	2.1703	2.1489	2.1074	2.0677	2.0315	2.0152
2	1.8912	1.8923	1.8954	1.9009	1.9136	1.9196	1.9337	1.9514	1.9733	1.9861
3	1.3174	1.3133	1.3011	1.2803	1.2339	1.2130	1.1672	1.1149	1.0583	1.0292
4	1.0000	1.0000	1.0000	1.0000	1.0000	1.0000	1.0000	1.0000	1.0000	1.0000
5	1.0000	1.0000	1.0000	1.0000	1.0000	1.0000	1.0000	1.0000	1.0000	1.0000
6	.7046	.7084	.7196	.7386	.7805	.7994	.8410	.8892	.9428	.9711
7	- .7046	- .7084	- .7196	- .7386	- .7805	- .7994	- .8410	- .8892	- .9428	- .9711
8	-1.0000	-1.0000	-1.0000	-1.0000	-1.0000	-1.0000	-1.0000	-1.0000	-1.0000	-1.0000
9	-1.0000	-1.0000	-1.0000	-1.0000	-1.0000	-1.0000	-1.0000	-1.0000	-1.0000	-1.0000
10	-1.3174	-1.3174	-1.3011	-1.2803	-1.2339	-1.2130	-1.1672	-1.1749	-1.0583	-1.0292
11	-1.8912	-1.8922	-1.8954	-1.9009	-1.9136	-1.9196	-1.9337	-1.9514	-1.9733	-1.9861
12	-2.2784	-2.2721	-2.2539	-2.2252	-2.1703	-2.1489	-2.1074	-2.0677	-2.0315	-2.0152

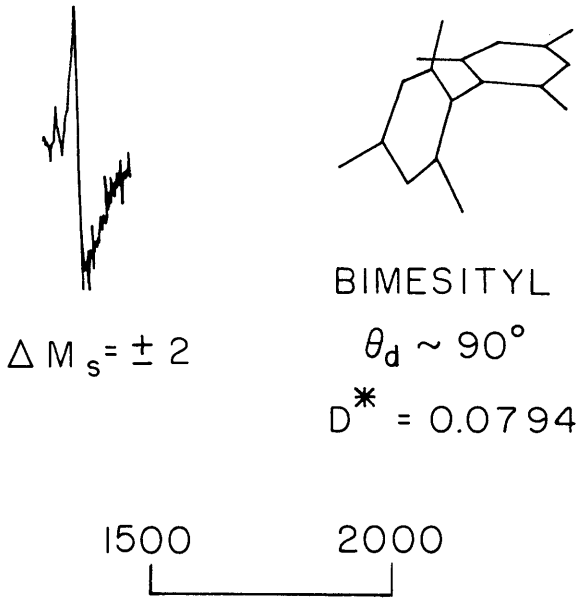

Fig. VII-10. Electron magnetic resonance spectrum, $\Delta M_s = \pm 2$ field, of bimesytyl.

in which two planar units are necessarily almost orthogonal, is consistent with the predicted trend that the absence of $\Delta M_s = \pm 1$ canonical field and the very weak $\Delta M_s = \pm 2$ H_{min} field reflect the shorter lifetime of the triplet state, that of two benzene-like systems.

B. S. Yamanashi

References

1. H. F. Hameka, Advanced Quantum Chemistry (Addison-Wesley Press, Inc., New York, 1965).
2. J. H. Van der Waals and M. S. de Groot, "Magnetic Interactions Related to Phosphorescence," in The Triplet State (Cambridge University Press, London, 1967), p. 101.
3. C. A. Hutchison, Jr., "Magnetic Resonance Spectra of Organic Molecules in Triplet States in Single Crystals," in The Triplet State, op. cit., p. 63.
4. J. H. Van Vleck, Rev. Mod. Phys. 23, 213 (1951).
5. M. Godfrey, C. W. Kern, and M. Karplus, J. Chem. Phys. 44, 4459 (1966).
6. H. Suzuki, Electronic Absorption Spectra and Geometry of Organic Molecules (Academic Press, Inc., New York, 1967), see Chap. 12.
7. M. Gouterman and W. Moffit, J. Chem. Phys. 30, 1107 (1959).
8. R. McWeeny, J. Chem. Phys. 34, 399 (1961).
9. Y. N. Chiu, J. Chem. Phys. 39, 2736 (1963).

B. CHARGE TRANSFER

1. Introduction

The nature of the interaction between the donor (cation) and the acceptor (anion) molecules that comprise a charge-transfer complex has never been clearly demonstrated. Following the theoretical treatment of charge transfer by R. S. Mulliken,[1] numerous spectroscopic and thermodynamic studies have appeared.[2,3] Until the present time, however, infrared, ultraviolet, nuclear magnetic resonance (NMR) and electron spin resonance (ESR) experiments have failed to elucidate the character of donor-acceptor (D-A) interaction in charge-transfer (C-T) complexes in solution. More successful x-ray crystallographic and ESR studies of solid C-T complexes have appeared,[4-7] which describe the geometric relationship between D and A molecules and also discuss electron distributions and mobility.

In this laboratory a system has been developed whereby solutions of donor and acceptor molecules are flowed together directly above the ESR cavity, and the ESR spectrum of the complex may be recorded immediately upon formation (flowing) or throughout any time period after formation (not flowing). Moreover, the D and A solutions may be subjected to electrolysis, thereby allowing observation of the following equilibrium situation from right to left, rather than left to right:

$$D + A \underset{k_2}{\overset{k_1}{\rightleftharpoons}} D^+A^- \underset{k_4}{\overset{k_3}{\rightleftharpoons}} D^+ + A^-.$$

The extent of formation and dissociation of the complex D^+A^-, that is, k_1, k_2, k_3, k_4, probably differs from solvent to solvent for a given complex, and, of course, from complex to complex, depending upon the relative donor and acceptor abilities (ionization potential and electron affinity) of the constituent molecules. It is the nature of bonding in D^+A^-, the complex, which this method demonstrates.

2. Apparatus

The instrument used is a Varian E-3 ESR spectrometer. The flow system has the following parts.

1. Two 1-l stainless-steel vacuum-tight tanks equipped with entry and exit stopcocks, in which D and A solutions are separately degassed by repeated freeze-pump-thaw cycles, and from which the solutions are flowed into the electrolytic cells.

2. Two 200-ml electrolytic cells, made up of an outer conical Pyrex chamber containing a tungsten electrode making contact with a mercury pool of large surface area, and an inner cylindrical chamber containing a platinum disk electrode. The inner and outer chambers are separated by a coarse fritted glass disk; liquid flow occurs between

them through a small hole in the side of the inner chamber. The solutions leave the outer chamber by means of a Pyrex exit tube that extends just above the level of the mercury pool.

3. Two exit tubes described above, through which flow is controlled and which meet above a teflon stopcock. It is here that the solutions mix.

4. One spectrosil quartz tube (3 mm O. D. for room temperature work, 2 mm O. D. for low-temperature work) connected to the flow system by means of a ball and socket joint. This quartz tube fits through the center of the cavity of the Varian E-3 ESR spectrometer.

5. One needle valve, located below the ESR cavity, which ultimately controls the flow rate.

The entire system is maintained under a positive pressure of N_2. This and the degassing of solutions mentioned above, eliminate dissolved O_2, which might otherwise cause broadening of ESR linewidths and might hinder electrolysis.

3. Materials

a. Donor

p-phenylenediamine (PPD): crude PPD is recrystallized three times from benzene and sublimed in vacuo at 150°C.

b. Acceptors

Tetracyanoethylene (TCNE): crude TCNE is recrystallized three times from chlorobenzene and sublimed in vacuo at 140°C.

2, 3-dichloro-5, 6-dicyano-1, 4-benzoquinone (DDQ): DDQ (Aldrich) is used without further purification. (The purity of all materials is attested to by the EPR spectra obtained.)

c. Solvents

Acetonitrile: acetonitrile is refluxed over P_2O_5 for 24 hours and then distilled through a helix-packed column. Early fractions are discarded.

Dimethoxyethane (DME): DME is refluxed over Na-K alloy and distilled in the same manner as acetonitrile.

d. Electrolyte

Tetra-N-butylammonium perchlorate (TNB): TNB is prepared from tetra-N-butylammonium hydroxide titrant (Eastman, 25% in methanol) by the addition of perchloric acid to an aqueous solution of the titrant. The white precipitate thus formed is washed with water, recrystallized from acetone, and dried in vacuo.

4. Experimental Results

When neutral (that is, not electrolyzed to produce anion or cation species) solutions of PPD and DDQ in acetronitrile are flowed together in the system described above, 3 superimposed spectra are obtained: two of the spectra are identical with those obtained for PPD^+ and DDQ^-, respectively, when each is produced separately by electrolytic oxidation or reduction. The third spectrum, however, can be accounted for by neither of the species mentioned above, and is therefore assumed to be the spectrum of the charge-transfer complex PPD^+-DDQ^-. The formation of such a complex is also indicated by a striking color change upon mixing of colorless PPD in acetonitrile and yellow DDQ in acetonitrile.

The hyperfine splitting constant of the DDQ-spectrum increases in the complexed anion by 15% over that of the uncomplexed anion. A further smaller spectral change occurs in the hyperfine splitting constants of PPD^+. Complete analysis of the new spectrum, whose total width is ~9 G and contains at least 16 lines, will be made when (i) a better resolved spectrum is obtained, and (ii) a computerized subtraction of the central, most intense DDQ five-line spectrum from the new spectrum is effected. The DDQ spectrum obscures approximately 50% of the new spectrum, at its center.

It is interesting to note that the PPD^+ spectrum decays rapidly, so that in a period less than 30 min, it is no longer distinguishable above the instrumental noise level. This decay may be explained by the relative instability of the PPD cation and may account for the appearance of only the anion species in earlier C-T studies. In these studies a solution was prepared containing donor and acceptor molecules. This solution was then degassed and studied, but a period greater than 15 min elapsed between the preparation of the solution and the observation of its spectrum.

The system PPD-TCNE has also been studied, in both acetonitrile and dimethoxyethane. In neither solvent was a new species observed, however.

4. Conclusions

These results demonstrate the potential usefulness of ESR spectrometry in the study of C-T complexes in solution. By observing and analyzing changes in the ESR spectra of donor and acceptor ions and by observing and analyzing the spectra of new species, it should be possible to quantitatively treat the nature of the interaction between the molecules comprising charge-transfer complexes.

Nancy H. Kolodny

References

1. R. S. Mulliken, J. Am. Chem. Soc. 74, 811 (1952); also see all subsequent papers in this series.

2. R. S. Mulliken, and W. B. Person, Ann. Rev. Phys. Chem. 13, 107 (1962); cf. all references.

3. E. M. Kossower, Progr. Phys. Org. Chem. 3, 81 (1965); cf. all references.
4. D. B. Chesnut and W. D. Phillips, J. Chem. Phys. 35, 1002 (1961).
5. D. B. Chesnut and P. Arthur, Jr., J. Chem. Phys. 36, 2969 (1962).
6. M. T. Jones and D. B. Chesnut, J. Chem. Phys. 38, 1311 (1963).
7. M. T. Jones and D. B. Chesnut, J. Chem. Phys. 40, 1837 (1964).